

1 **A novel DNA-based *in situ* hybridization method to detect *Desmozoon lepeophtherii* in**
2 **Atlantic salmon tissues**

3

4 Running title: *In situ* hybridization to detect *Desmozoon lepeophtherii*

5

6 Ana Herrero^{1*}, Oswaldo Palenzuela^{2*}, Hamish Rodger³, Chris Matthews⁴, Mar Marcos-

7 López⁴, James E. Bron⁵, Mark P. Dagleish¹ and Kim D. Thompson¹

8

9 ¹More dun Research Institute, Pentlands Science Park, UK

10 ²Institute of Aquaculture, Torre de la Sal (IATS-CSIC), Castellón, Spain

11 ³VAI Consulting, Kinvara, Co. Galway, Ireland

12 ⁴PHARMAQ Analytic, Inverness, UK

13 ⁵Institute of Aquaculture, University of Stirling, Stirling, UK

14

15 * These authors contributed equally to this work.

16 Correspondence: Email: anaherrerfern@gmail.com. Ana Herrero present address is VAI

17 Consulting, Kinvara, Co. Galway, Ireland.

18

19 **ORCID**

20 Ana Herrero- 0000-0002-2484-2769

21 Oswaldo Palenzuela - 0000-0001-7702-6098

22 Hamish Rodger - 0000-0002-5336-8912

23 James E Bron - 0000-0003-3544-0519

24 Mark P. Dagleish - 0000-0001-6909-6467

25 Kim D. Thompson - 0000-0003-3550-4842

26 **ACKNOWLEDGMENTS**

27 We would like to thank Simon Jones for providing gill tissue from farmed Atlantic salmon
28 from Canada infected with *D. lepeophtherii*.

29

30 **DATA AVAILABILITY STATEMENT**

31 The datasets generated during and/or analysed during the current study are available from
32 the corresponding author on reasonable request.

33

34 **FUNDING STATEMENT**

35 This work was supported financially by the European Commission under the TNA
36 programme within AQUAEXCEL²⁰²⁰ project, IATS-CSIC as hosting institution, Moredun
37 Research Institute and Vet-Aqua International.

38

39 **CONFLICT OF INTEREST**

40 The authors declare that there are no potential sources of conflict of interest with this work.

41

42 **ETHICAL APPROVAL**

43 NA

44

45

46

47

48

49

50

51 **ABSTRACT**

52 The microsporidian *Desmozoon lepeophtherii* Freeman and Sommerville, 2009 is
53 considered significant in the pathogenesis of gill disease in Atlantic salmon (*Salmo salar*
54 Linnaeus, 1758). Due to the difficulty in detecting *D. lepeophtherii* in tissue sections,
55 infections are normally diagnosed by molecular methods, routine haematoxylin and eosin
56 (H&E) stained gill tissue sections and the use of other histochemical stains and labels to
57 confirm the presence of spores. An *in situ* hybridization (ISH) protocol specific for *D.*
58 *lepeophtherii* was developed using DIG-labelled oligonucleotide probes. Diseased Atlantic
59 salmon gills, were analysed by ISH, calcofluor white (CW) and H&E. All methods showed
60 high levels of specificity (100%) in their ability to detect *D. lepeophtherii*, but the
61 sensitivity was higher with ISH (92%), compared with CW (64%) and presence of
62 microvesicles on H&E stained sections (52%). High levels of *D. lepeophtherii* spores were
63 significantly associated ($p < 0.05$) with the development of *D. lepeophtherii*-associated
64 pathology in the gills, with Ct values below 19 and over 100 microsporidia/10 mm² of gill
65 tissue (from the ISH counts) seemingly necessary for the development of microvesicles.
66 The ISH method has the advantage over other histological techniques in that it allows all
67 life-stages of the microsporidian to be detected in infected salmon gill tissue sections.

68

69

70

71

72 **KEYWORDS:** *Desmozoon lepeophtherii*; *Paranucleospora theridion*; microsporidian, gill
73 disease; ISH

74 **1. INTRODUCTION**

75 The microsporidian *Desmozoon lepeophtherii* Freeman and Sommerville, 2009 (syn.
76 *Paranucleospora theridion*) is one of the most prevalent agents detected by polymerase
77 chain reaction (PCR)-based assays in the gills of marine farmed Atlantic salmon (*Salmo*
78 *salar* Linnaeus, 1758) in Europe, irrespective of the health status of the fish (Downes et al.,
79 2018; Gjessing et al., 2019; Steinum et al., 2010). Higher burdens of *D. lepeophtherii* have
80 been observed in the gills of Atlantic salmon during the autumn months (Gunnarsson et al.,
81 2017), the season in which outbreaks of gill disease associated with *D. lepeophtherii* are
82 usually reported (Matthews et al., 2013; Weli et al., 2017). From gross examination, gills
83 affected by *D. lepeophtherii* present with areas of paleness and swollen filaments (pers. obs.).
84 Histologically, gill lesions associated with the microsporidian include necrosis, hypertrophy
85 and hyperplasia of the lamellar epithelial cells, infiltration by phagocytic cells and cell debris
86 with associated pigmented material (Matthews et al., 2013; Gjessing et al., 2019). However,
87 the pathology changes through the course of the disease. Matthews et al. (2013) described a
88 *D. lepeophtherii* infection in farmed Atlantic salmon in Scotland with findings including
89 lamellar epithelial cell proliferation, infiltration by inflammatory cells and the presence of
90 necrotic and hypertrophied gill epithelial cells in association with the presence of
91 microsporidian spores. Fish sampled one week later had less severe inflammatory cell
92 infiltrate and necrotic lesions and fewer *D. lepeophtherii* spores present in the gills but
93 prominent lamellar epithelium hyperplasia and hypertrophy was still present. Weli et al.
94 (2017) reported *D. lepeophtherii* to be the main cause for the clinical disease observed in
95 gills during a longitudinal study of Norwegian farmed Atlantic salmon. Necrotic lesions
96 were more severe during the acute stage of the disease (during early sampling time points),
97 while chronic pathology (present during later sampling time points) was characterised by a

98 marked host response, including severe inflammatory cell infiltration and hyperplasia of the
99 gill epithelium.

100 The life cycle of *D. lepeophtherii* is complex: one type of sporogony occurs in the
101 sea lice (*Lepeophtheirus salmonis* Kroyer, 1837) and two different presumptive
102 developmental cycles occur in salmon (Nylund et al., 2010). In salmon two different types
103 of spores develop (Nylund et al., 2010): (1) auto-infective ~ 1 µm-diameter oval/spherical
104 intracytoplasmic spores and (2) environmental ~ 2.5 µm-long x 2.0 µm-wide ellipsoidal
105 intranuclear spores. Matthews et al. (2013) improved the sensitivity of detecting the small
106 *D. lepeophtherii* auto-infective spores in salmon gills by using the Gram Twort stain.
107 However, the technique severely under-estimates the total number of spores compared to
108 other methods, such as staining with calcofluor-white (CW) or labelling by
109 immunohistochemistry (IHC) (Herrero et al., 2020). Additionally, none of these methods
110 facilitates the detection of the other pre-sporogonic stages of *D. lepeophtherii* which can be
111 present. An *in situ* hybridisation (ISH) method was developed to detect *D. lepeophtherii*
112 based on a large plasmid-encoded RNA probe (Weli et al., 2017). However, this method
113 has practical difficulties due to lack of reproducibility in generating the probe, balancing
114 the preservation of tissue morphology against adequate probe permeability and the labile
115 nature of the RNA probe (Corthell, 2014).

116 In outbreaks of complex gill disease, which is caused by multiple aetiological agents
117 (Herrero et al., 2018), the lesions caused by each individual agent can be difficult to
118 differentiate, including those caused by *D. lepeophtherii*. Additionally, the high prevalence
119 of the microsporidian in salmon populations, the rapid change in the progression of the
120 pathology and the difficulty of detecting the parasite with histochemical stains make the
121 study of gill disease associated with this organism challenging. A more sensitive and
122 specific method capable of detecting all stages of the parasite's life cycle, not just the

123 spores, would allow accurate detection of *D. lepeophtherii* and help gain insight into its
124 specific histological lesions. *In situ* hybridisation has been used to successfully detect and
125 visualise pre-sporogonic and sporogonic stages of the microsporidia *Enterospora*
126 *nucleophila* Palenzuela et al., 2014 and *Nucleospora salmonis* Chilmonczyk et al., 1991
127 using probes against the small subunit ribosomal RNA (SSU rRNA) or intergenic regions
128 of the rRNA, respectively (Ahmed et al., 2019; Grésotiac et al., 2007). Probes were applied
129 to formalin fixed, paraffin-wax embedded (FFPE) tissue samples and resulted in more
130 sensitive detection of the parasite compared with histochemical stains. A RNAScope® ISH
131 protocol for the detection of multiple different targets, including *D. lepeophtherii*, was also
132 used in a recent investigation of bacterial, viral and parasitic agents in complex gill disease
133 of Atlantic salmon (Gjessing et al., 2021). This procedure, however, used proprietary
134 probes whose specificity is difficult to assess.

135 The aim of this study was to develop and optimise an ISH protocol using DNA
136 oligonucleotide probes for the species-specific detection of all life-stages of *D.*
137 *lepeophtherii* in tissue sections which could be practical for research and diagnostic
138 purposes. The detection of the parasite in infected tissue sections and associated pathology
139 were compared with other histological staining methods, the results of which were
140 correlated with *D. lepeophtherii* specific real-time reverse transcriptase PCR (RT-rtPCR).

141

142 **2. MATERIALS AND METHODS**

143 **2.1 Samples used in the study**

144 Archived marine stage Atlantic salmon gill tissue samples (n=28) obtained from farms
145 located on the west coast of Scotland and collected between 2016 and 2017 were provided
146 by PHARMAQ Analytiq (Inverness, Scotland). Tissue sections from fish with different
147 burdens of *D. lepeophtherii* were selected for this study. All samples had been analysed

148 previously by RT-rtPCR, performed as described by Nylund et al. (2010), to quantify the
149 relative amounts of *D. lepeophtherii*-specific RNA in gill samples, expressed as Ct values
150 and presented in Supplementary Table 1. Samples positive for *D. lepeophtherii* by RT-
151 rtPCR were used as positive controls and gill tissues confirmed as *D. lepeophtherii*-free by
152 RT-rtPCR were used as negative controls to develop and validate the ISH protocol.

153 To test the specificity of the oligoprobes, tissue sections containing two closely
154 related species of microsporidia from the Enterocytozoonidae family, *Enterocytozoon*
155 *hepatopenaei* Tourtip et al., 2019 in the hepatopancreas of the black tiger shrimp (*Penaeus*
156 *monodon* Fabricius, 1798) and *N. cyclopteri* Freeman et al., 2013 in the kidney of the
157 lumpfish (*Cyclopterus lumpus* Linnaeus, 1758), were subjected to the ISH method.

158 Additional Atlantic salmon tissue sections used to optimise the ISH protocol
159 included heart, liver, stomach, pancreas, spleen, intestine, pyloric caeca, kidney, muscle
160 and skin. Other samples subjected to the ISH protocol included; a sea louse (*L. salmonis*)
161 from a salmon farm in Scotland that had xenomas under its cuticle suggestive of *D.*
162 *lepeophtherii* infection and gill tissue from farmed Atlantic salmon in Canada infected with
163 *D. lepeophtherii* that was positive by specific RT-rtPCR (kindly provided by Prof S. Jones,
164 Pacific Biological Station, Nanaimo, Canada).

165

166 **2.2 Development of a DNA oligoprobe ISH protocol to detect *D. lepeophtherii***

167 Oligonucleotide probes specific for *D. lepeophtherii* were designed by aligning all the
168 sequences of the microsporidian and phylogenetically close species available within the
169 SILVA database release 132 (Pruesse et al., 2007, www.arb-silva.de). The dataset was
170 mostly comprised of the SSU rRNA region, but some segments from the internal
171 transcribed spacer (ITS) and partial large subunit (LSU) regions were also inspected. The
172 alignment showed no significant sequence variations between genotypes from farmed

173 Atlantic salmon in Scotland or Norway, different species of sea lice (*Caligus elongatus*
174 Nordmann, 1832 and *L. salmonis*), ballan wrasse (*Labrus bergylta* Ascanius, 1767) or
175 rainbow trout (*Oncorhynchus mykiss* Walbaum, 1792). Variation was observed between
176 the Canadian and European genotypes of *D. lepeophtherii*, as reported previously by Jones
177 et al. (2012). The alignment was pruned to the longest representative genotypes available
178 for *D. lepeophtherii* and closely related Enterocytozoonidae microsporidia (Table 1).
179 Regions showing sufficient variability between the genotypes of *D. lepeophtherii* and the
180 closely related species were chosen to design appropriate antisense oligonucleotide
181 probes. *In silico* analyses of the thermodynamic profiles and specificity were aided by the
182 software package OLIGO 7 (Rychlik, 2007) and by NCBI BLAST search tools
183 (<http://blast.ncbi.nlm.nih.gov/Blast.cgi>). The five *D. lepeophtherii*-specific antisense
184 oligonucleotide probes targeting the regions SSU rRNA (n = 3) and ITS (n = 2) designed
185 for use in this study are presented in Table 2. Oligoprobes were synthesised and labelled
186 with digoxigenin deoxyuridine triphosphate (DIG-dUTP) at the 5' and 3' ends of the
187 probes (Eurofins Genomics, Ebersberg, Germany).

188 The ISH protocol was based on the method described by Palenzuela and
189 Bartholomew (2002), with modifications. Formalin fixed, paraffin-wax embedded gill
190 tissue samples were sectioned (4 µm), mounted on Superfrost plus coated slides (Menzel-
191 Gläser, Braunschweig, Germany) and incubated at 60°C for 1 h. Sections were dewaxed
192 in xylene, rehydrated through a decreasing ethanol concentration (100%, 95% and 70%)
193 and then equilibrated in Tris-CaCl₂ buffer (200mM Tris, 2mM CaCl₂, pH 7.2) for 10 min.
194 As *D. lepeophtherii* is an intracellular pathogen, permeabilisation of the tissue was
195 performed to allow intracellular penetration of the probes to improve binding to their target
196 sequence. To optimise this procedure, serial sections were permeabilised with proteinase
197 K (PK) (Roche, Welwyn, UK), 15 µg mL⁻¹ in Tris-CaCl₂, for 10 and 30 min at 37°C.

198 Tissues not exposed to PK were also examined. Proteolysis was stopped with two washes
199 in 2x saline-sodium citrate buffer (SSC) (0.3 M NaCl buffer, 0.03 M trisodium citrate, pH
200 7.0) for 10 min each. Slides were covered with 400 μ L of freshly made hybridization
201 mixture consisting of 112 μ L nuclease-free water, 40 μ L of 20x SSC buffer (3.0 M NaCl
202 buffer, 0.3 M trisodium citrate, pH 7.0), 100 μ L of deionized formamide (Sigma-Aldrich),
203 8 μ l Denhardt's solution, 80 μ l dextran sulphate (50%, w/v) (Sigma-Aldrich), 40 μ L of
204 10x PBS and 20 μ L of DNA from fish sperm (MB- grade, Sigma-Aldrich). DIG-labelled
205 oligoprobe concentrations were adjusted to 100mM with Tris-EDTA buffer (TE). Equal
206 concentrations of different probes were mixed together to make two cocktails. Cocktail 1
207 (C1) comprised probes 16L21, 819L25 and 1339L25. Cocktail 2 (C2) comprised probes
208 1284L21, 1002L25 and 1339L25. Both cocktails were prepared at various dilutions
209 (1/1000, 1/500 and 1/200) in hybridization buffer. Each oligonucleotide probe (1/1000
210 dilution) was also tested individually on serial sections. Slides with the probes applied
211 were placed on a heating block at 95°C for 10 min. After two min at this temperature,
212 slides were covered with Hybri-slips (Sigma-Aldrich) and incubated at 37°C overnight to
213 hybridize to complementary sequences. After overnight incubation, slides were rinsed
214 with 2x SSC buffer to remove the Hybri-slip. Stringency washes were then performed,
215 using 2x 10 min washes in 2x SSC buffer, to remove any unbound probes and assessed at
216 two different temperatures, 37°C and 45°C, 2x 10 min in 1x SSC buffer at 37°C and,
217 finally, once in 0.25x SSC buffer for 10 min at 37°C for C1. The same wash procedure
218 was used for slides incubated with C2, except for the last stringency wash which was
219 performed with 0.5x SSC buffer for 10 min, again assessing at two different temperatures,
220 37°C and 45°C. The slides were shaken slowly during each wash. Following the stringency
221 washes, the tissue sections were transferred to wash buffer A (1 M Tris base, 1.5 M NaCl,
222 pH 7.5) for 10 min at 24°C. Subsequent to this, sections were incubated for 1 h at 21°C

223 with blocking solution (2% sheep serum, 0.1% Triton X-100 in wash buffer A) to prevent
224 non-specific antibody binding. Bound probes were detected by covering the slides with a
225 commercial sheep anti-DIG antibody (Fab fragments) conjugated to alkaline phosphatase
226 (AP) (Roche, Manheim, Germany, reference 11093274910) diluted 1:200 in blocking
227 solution for 2h at 21°C. Unbound antibody was removed using wash buffer A for 2 x 10
228 min and then incubating in wash Buffer B (100 mM Tris, 100 mM, NaCl, 50 mM, MgCl₂,
229 pH 9.5) for 10 min, with agitation, at 21°C. The reaction development was optimised by
230 incubating the slides for either 3 h or overnight with AP enzyme substrate NBT/ BCIP (5-
231 bromo-4-chloro-3-indolyl phosphate and 4-nitro-blue tetrazolium chloride) (Roche),
232 diluted 1:500 in wash Buffer B, without MgCl₂, at 21°C in the dark. The visualisation
233 reaction was terminated by placing the sections in wash buffer A for 10 min.

234 Sections were counterstained with light green (1%) (AtomScientific, Manchester,
235 UK) for 4 min, and transferred to a solution of 0.05 % acetic acid in acetone for 1 min.
236 Sections were dipped 10 times in distilled water, dehydrated through increasing
237 concentrations of ethanol (96% and 100%), cleared in xylene and mounted using
238 VectaMount (Vector Laboratories, Burlingame, CA, USA).

239

240 **2.3 Comparison of the ISH method with other techniques**

241 Atlantic salmon FFPE gill tissue samples were sectioned (4 µm) sequentially and adjacent
242 sections stained with H&E (Stevens and Wilson, 1996) and CW (Fluka, Buchs,
243 Switzerland) (Herrero et al., 2020), as well as using the optimised ISH protocol. All sections
244 were examined with an Olympus BX51 microscope (Olympus, Southend-on-Sea, UK) and
245 photomicrographs were taken with an Olympus DP70 Digital Camera System (Olympus)
246 using analySiS[®] software (Olympus).

247 To quantify the number of microsporidia visible in the gill sections, each section
248 was examined using a 20x objective lens over a 10 mm² tissue area to determine the number
249 of *D. lepeophtherii* positive structures labelled.

250

251 **2.4 Assessment of *D. lepeophtherii* presumptive pathology**

252 The characteristic lesions in hypertrophied and necrotic epithelial cells associated with the
253 presence of *D. lepeophtherii* in infected salmon gill tissues have been termed
254 “microvesicles” (Weli *et al.*, 2017). The severity of microvesicle/necrosis score (MV/N) on
255 H&E stained sections was scored from 0 to 3: 0 = absence of pathology suggestive of *D.*
256 *lepeophtherii*, 1 = foci of epithelial cell necrosis (Supplementary Figure 1a) but no obvious
257 *D. lepeophtherii*-related microvesicles, 2 = a small to medium number of microvesicles
258 typical of *D. lepeophtherii* infection, 3 = a large number of microvesicles typical of *D.*
259 *lepeophtherii* infection present in the gill epithelial cells (Supplementary Figure 1b).

260

261 **2.5 Statistical analyses**

262 Sensitivity, specificity, positive predictive value and negative predictive value were
263 calculated according to Martin (1977), taking RT-rtPCR results as a reference (Table 3).
264 The data were not normally distributed (Shapiro-Wilk’s test) and Spearman rank correlation
265 coefficients were calculated to determine any correlations between the MV/N-H&E score
266 and the Ct values obtained by RT-rtPCR, and between the MV/N-H&E score and the total
267 ISH counts observed in the gill tissue. The Pearson's correlation coefficient test was used
268 to examine correlations between the total ISH counts observed in the gill tissue with the Ct
269 values obtained. Statistical significance was set at $p \leq 0.05$ and all statistical analyses were
270 performed using R (R software, v. 3.5.3; <https://www.r-project.org/>)

271

272 **3. RESULTS**

273 **3.1 Development and optimisation of the ISH technique**

274 The influence of different concentrations of reagents and variation in incubation times on
275 the success of the ISH protocol are summarised in Table 4. Permeabilization of the tissue
276 with PK for 10 min compared to 30 min gave the same level of labelling of *D. lepeophtherii*,
277 but the tissue morphology was less disrupted after incubation with PK for 10 min, so this
278 was used. Also, omission of the pre-hybridisation step did not affect the results. Cocktail 1
279 gave slightly more background signal compared to Cocktail 2, although this difference
280 decreased with more stringent washing, i.e. using SSC buffer at 0.25x to remove unbound
281 probes after using Cocktail 1. The optimum dilution of the probes was 1/1000 for both
282 Cocktail 1 and Cocktail 2, with higher concentrations of probes giving no increased signal
283 in the tissue sections. A 3 h incubation time with the AP enzyme substrate was sufficient to
284 produce an optimal labelling, whereas the reaction was over-developed when applied
285 overnight. The final optimised protocol was used to test the probes separately. Probes
286 targeting the SSU rRNA (16L21, 819L25, and 1002L25) produced a strong signal, with
287 some background present using probe 819L25 (Table 2). Probes targeting the ITS region
288 gave different results. Probe 1339L25 gave a good signal whilst probe 1284L21 was the
289 only probe tested that did not show any labelling (Table 2).

290

291 **3.2 Detection of *D. lepeophtherii* in Atlantic salmon gills using ISH**

292 Successful binding of the probes to the *D. lepeophtherii* target sequences was denoted by
293 a dark blue-purple signal, depicting the presence of the parasite, against a light green
294 counterstain (Figure 1). All negative control preparations were devoid of any blue-purple
295 signal (Figure 1a). Proliferative stages of *D. lepeophtherii*, i.e. pre-sporogonic structures
296 and possibly meronts, appeared as intensely blue-purple labelled round structures

297 approximately 4-6 μm in diameter (Figure 1b & 1c) and were present most frequently in
298 the cytoplasm of gill epithelial and blood vessel endothelial cells. Sporont-like structures
299 appeared as a vacuole containing multiple punctate blue-purple inclusions, and were
300 considered to be immature spores (Figures 1d).

301 Both types of spores, auto-infective and environmental, although less consistently
302 labelled than the pre-sporogonic structures were still visibly discernible in the gills. Auto-
303 infective spores were smaller, approximately 0.8-1.0 μm in diameter, and appeared,
304 typically, in clusters in the cytoplasm of gill epithelial cells. These spores did not always
305 appear as complete structures, but were denoted by small punctate labelling in necrotic
306 tissue (Figure 2a). Environmental spores were larger (2.0-2.5 μm) and present in the
307 nucleus of gill epithelial cells or associated with necrotic epithelial cells (Figure 2b).
308 Spores were generally less intensely labelled than pre-sporogonic stages and variation in
309 the intensity was noted also (Figure 2c).

310 **3.3 Detection of *D. lepeophtherii* in non-gill tissues and probe specificity**

311 Tissues from the RT-rtPCR-positive fish also showed labelling for *D. lepeophtherii* by ISH
312 in the kidney interstitium (Figure 3a), the parenchyma of the spleen and liver and *lamina*
313 *propria* of the intestine (Figure 3b). Sections of sea lice containing typical xenoma-like
314 structures, caused by *D. lepeophtherii*, were also ISH positive, with multiple foci of
315 microsporidia labelled (Figure 3c). The gills of Atlantic salmon from the Canadian fish
316 farm showed similar labelling to those from Scottish farms using the probes targeting the
317 SSU rRNA (Figure 3d), but no labelling was obtained with probes complementary to the
318 ITS region. The oligoprobes used in this study did not cross-react with any of closely related
319 microsporidian species examined (*N. cyclopteri* and *E. hepatopenaei*) as denoted by the
320 tissue sections containing them being devoid of any labelling after being subjected to the
321 ISH protocol.

322 **3.4 Comparison of ISH with other techniques used to identify *D. lepeophtherii***

323 Calcofluor white stained two different sizes of spores both of oval/spherical shape. The
324 smaller one (1.1 μm length) was present in the cytoplasm of cells along the lamellae, but
325 the specific cell types were difficult to identify due to the poor preservation of tissue
326 morphology associated with this technique. These smaller spores were mostly present in
327 aggregates of 3 to 20; when not present in aggregates a 60x objective lens was required to
328 visualise individual spores due to their low level of fluorescence (Figure 4).

329 Larger, oval, spores were clearly visible under a 20x objective due to their stronger
330 fluorescence signal and larger size ($\sim 2.5 \mu\text{m}$ -length). These were present singularly or in
331 pairs. It was unclear if they were located within the nucleus or the cytoplasm of the cells,
332 again, due to the poor preservation of tissue morphology that occurs with this technique.
333 Calcofluor white stained large (environmental) spores in gill tissue even when parasite
334 loads were low (as denoted by RT-rtPCR), but the smaller auto-infective spores were only
335 visible with CW when the total number of microsporidia labelled with ISH was high
336 ($\geq 150/10 \text{ mm}^2$).

337 Results for the 28 different sections of Atlantic salmon gills analysed using ISH,
338 CW and H&E (based on the presence of microvesicles) showed that all methods were
339 highly specific (100%) in their ability to detect *D. lepeophtherii* but that the sensitivity,
340 compared to RT-rtPCR, was markedly higher using the ISH technique (92%), followed by
341 CW (64%) and then H&E (52%) (Table 5). Positive predictive values (probability that
342 subjects with a positive screening test really have the disease) and negative predictive
343 value (probability that subjects with a negative screening test do not have the disease) are
344 also shown in Table 5.

345

346 **3.5 Gill *D. lepeophtherii* burden and the presence of microvesicles**

347 From the 25 *D. lepeophtherii* RT-rtPCR-positive fish examined, 6 were devoid of any
348 pathology suggestive of *D. lepeophtherii* infection (MV/N-H&E score 0). Presence of mild
349 to moderate, multifocal, lamellar epithelial cell necrosis (Figure 5) was present in 5 fish
350 (MV/N-H&E score-1). Low numbers of microvesicles, suggestive of *D. lepeophtherii*, were
351 present in 11 of the examined gill samples (MV/N-H&E score 2), and a large number
352 microvesicles were present in 3 fish (MV/N-H&E score 3). The presence of microvesicles
353 was mostly observed when the total number of *D. lepeophtherii* labelled by ISH was
354 between 120-850/10 mm² tissue in fish gill tissue, although one fish had a small number of
355 microvesicles present despite having only 30 ISH-positive *D. lepeophtherii* structures
356 (Figure 6). In agreement with this, the presence of microvesicles in gill tissue sections was
357 observed only when the *D. lepeophtherii* load was very high as determined by RT-rtPCR
358 (Ct ≤19). Swabs taken from gills and assessed by RT-rtPCR showed less consistent results
359 with respect to the presence of necrosis in the corresponding tissue sections when examined
360 histologically. The swab from fish 23 had a Ct value of 19 but was devoid of necrosis in
361 the corresponding gill tissue section stained with H&E, while the gill swab from fish 24
362 had a Ct value of 20 but had large numbers of microvesicles in its corresponding tissue
363 section, visible by H&E staining, suggestive of *D. lepeophtherii* infection.

364 Spearman rank correlation coefficient between the MV/N - H&E score and the total
365 ISH counts in the gill tissue was significant (rs= 0.89; 95% confidence interval; p < 0.001).
366 There was a significant correlation between the MV/N-H&E score and Ct values obtained
367 from gill biopsies (rs= -0.92; 95% confidence interval; p < 0.001), but there was no
368 correlation between the MV/N-H&E score and the Ct results obtained from gill swabs (rs=
369 0.69; 95% confidence interval; p= 0.056). When the total number of microsporidia labelled
370 with ISH was compared with all RT-rtPCR results (from gill biopsies and swabs) there was
371 a significant correlation (p ≤0.03), and between the ISH and the gill biopsy Ct value results

372 ($p \leq 0.03$). However, there was no correlation ($p = 0.22$) between the ISH scores and the Ct
373 results from gill swabs.

374

375 **4. DISCUSSION**

376 A total of five species-specific antisense DNA oligonucleotide probes were designed for *D.*
377 *lepeophtherii*, three complementary to the positive strand of the SSU and two to the ITS
378 region. Two of the three probes directed against the SSU and one to the ITS region gave a
379 strong positive signal in the ISH, while labelling with the other SSU probe, 819L25, did
380 not give clear visualisation of the parasite due to non-specific labelling. Reduction of the
381 non-specific labelling when using probe 819L25 was achieved by increasing the stringency
382 of washing steps (Wilcox, 1993) thereby removing effectively the all unbound probe. As
383 well as detecting *D. lepeophtherii* in the gills of farmed salmon from Europe, the four
384 functional probes also detected *D. lepeophtherii* in the gills of Canadian farmed salmon.
385 The only probe that did not label *D. lepeophtherii* was 1284L21, which had several
386 mismatches with the Canadian genotype as it was designed deliberately to discriminate (in
387 the ITS region) between the European and Canadian genotypes of *D. lepeophtherii*.
388 However, this design was based on only two available sequences representing both
389 genotypes and extending across the ITS and greater diversity may exist in *D. lepeophtherii*
390 genotypes at this locus. In the fungal kingdom, the ITS region has been shown to be
391 generally better for inter- and intraspecific discrimination compared to the LSU or SSU
392 (Schoch et al., 2012). For instance, more than 100 genotypes have been described for the
393 microsporidian *Enterocytozoon bieneusi*, a microsporidian closely related to *D.*
394 *lepeophtherii*, by sequence analysis of the ITS, and these various genotypes have been
395 associated with different host affinities and different levels of pathogenicity (Galván-Díaz
396 et al., 2014). Further molecular characterization of intraspecies genetic diversity between

397 *D. lepeophtherii* obtained from different geographical areas and host species may help in
398 understanding the role of this microsporidian species in gill disease.

399 The probes we developed for the ISH appear to be specific for *Desmozoon* spp. in
400 that they did not cross-react with the two related microsporidia examined (*E. hepatopenaei*
401 and *N. cyclopterii*). Also, the xenoma-like structures found below the cuticle of sea lice,
402 highly suggestive of a *D. lepeophtherii* infection (Freeman and Sommerville, 2009),
403 labelled intensely when screened with the ISH protocol confirming the presence of the
404 parasite. Therefore, the ISH will be a valuable tool for studying the various stages in the
405 life cycle of *D. lepeophtherii* both in sea lice and Atlantic salmon.

406 In the gill tissue, positive labelling, by ISH, of the parasite's developmental stages
407 was present in the cytoplasm and nuclei of the gill lamellar epithelial cells and in the
408 cytoplasm of endothelial cells of the blood vessels in the gills in agreement with the
409 described life cycle (Nylund et al., 2010) and previous studies (Weli et al., 2017). Small
410 auto-infective spores were sometimes present within the cytoplasm of apparently normal
411 gill lamellar epithelial cells, in the absence of pathology, while larger environmental
412 spores were occasionally observed within nuclei of gill lamellar epithelial cells, or
413 associated with degenerate epithelial cells, and both spore types had variable and less
414 intense labelling compared to the pre-sporogonic stages. Limitations of ISH in detecting
415 spores are reported frequently and considered to be due the predicted lower number of
416 targets and the low permeability of microsporidian spore stages to probes (Ahmed et al.,
417 2019). Additionally, the detection of microsporidia with ISH using antisense DNA
418 oligonucleotides that target the SSU region may result in a poor spore signal due to reduced
419 or absent target protein synthesis during the spore stage and the highly condensed genome
420 of some microsporidian species which could reduce the availability to the probes of the
421 target regions in the parasite's genomic rDNA. This reduced intensity of labelling of

422 spores by ISH has been reported for other microsporidian species including a RNA-based
423 ISH method for detecting *D. lepeophtherii* (Weli et al., 2017). In our procedure, spores
424 were identified mainly as punctate labelling and rarely as fully labelled oval structures.
425 However, the increased intensity of ISH spore signal in this study compared to other
426 studies could be due to the use of the 5'-, 3'-doubly labelled probes employed instead of
427 the more typical singly labelled probes. This approach has proven successful in other
428 studies (Stoecker et al., 2010).

429 Although a description of the parasite's systemic distribution and associated
430 pathology was not the aim of this study, fish with high burdens of *D. lepeophtherii* in the
431 gills (by ISH signal or RT-rtPCR values) showed a positive ISH signal in other organs.
432 *Desmozoon lepeophtherii* was first detected in salmon tissue by conventional PCR in the
433 kidney, liver, gills and circulating blood cells from (clinically normal) farmed Atlantic
434 salmon in Scotland (Freeman, 2002). Later, Nylund et al. (2010) detected developmental
435 stages of the parasite in the blood vessel endothelial cells and the cytoplasm of leukocytes
436 by transmission electron microscopy. The systemic distribution of the microsporidian has
437 been reported by others (Matthews et al., 2013; Nylund et al., 2011) but has not been
438 associated with major tissue damage with the exception of one case report in which the
439 presence of *D. lepeophtherii* was associated with severe pathology in the gills, peritoneal
440 cavity and the gastrointestinal tract (Weli et al., 2017). In our study, only low levels of *D.*
441 *lepeophtherii* were detected in the gastrointestinal epithelium. However, we only used
442 single or small groups of fish from different clinical cases, which may not have had the
443 same clinical signs as those reported by Weli et al. (2017). Little is known about the effects
444 of *D. lepeophtherii* in the other organs of fish and its systemic distribution has generally
445 been overlooked.

446 Analysis of the sensitivity and specificity of the ISH protocol allowed comparison
447 with other detection methods. Complete clinical validation of this ISH method would
448 require the analysis of samples from a large population of *D. lepeophtherii*-infected vs.
449 non-infected fish (Georgiadis et al., 1998). Unfortunately, sampling of the required
450 magnitude was outwith the scope of the present study. In addition, the peak incidence of
451 clinical disease is usually seasonal and short (Matthews et al., 2013), and a large number
452 of tissue samples from fish with typical gross pathology would be challenging to collect.
453 However, gill samples from 28 fish subjected to the ISH protocol allowed initial
454 comparison with other histological methods (CW and H&E) commonly used to detect *D.*
455 *lepeophtherii*. Tissue sections containing various parasite loads were selected based on
456 RT-rtPCR results, used as a 'gold standard positive control'. The sensitivity of the ISH
457 protocol was high (92%) when compared to RT-rtPCR. As both techniques target the
458 genome of the microsporidian, both the PCR and the ISH are capable of detecting levels
459 associated with subclinical as well as clinical infections that can be missed by other, less
460 sensitive, histological methods. Although RT-rtPCR is more sensitive than ISH, because
461 of the amplification of the original signal, it is susceptible to false positive results due to
462 contamination. The ISH protocol combines the high sensitivity and specificity of
463 molecular detection with direct observation of the presence, subjective load and
464 distribution of the parasite, including the severity and morphology of histological lesions
465 in the gill tissue and parasite lesion-association. Furthermore, when gill biopsies were
466 subjected to RT-rtPCR, the Ct values obtained correlated significantly with the total
467 number of parasites observed in the gill tissue using ISH. However, no correlation was
468 found between RT-rtPCR Ct values derived from gill swabs and the ISH of the
469 corresponding gill tissue. These results highlight the usefulness of ISH for quantifying the
470 parasite level and for determining the parasite-associated pathology in the gills, which

471 facilitates the understanding of the role of *D. lepeophtherii* in gill disease. Additionally,
472 due to its high specificity and sensitivity the ISH method can be used as a standalone
473 procedure in the absence of RT-rtPCR results. Although gill swabbing is a minimally
474 invasive option for assessing the presence of the microsporidian in fish gills by RT-rtPCR,
475 our results show using gill swabs is less reliable than using gill tissue, probably because
476 of the intracellular nature of the parasite.

477 Calcofluor white allowed the visualization of the two types of spores described for
478 *D. lepeophtherii* (Nylund et al., 2010), in agreement with previous studies (Herrero et al.,
479 2020; Weli et al., 2017), and has been widely used to detect microsporidia (Luna et al.,
480 1995). This is due to its ability to bind to chitin present on the inner layer of the spore wall
481 and its greater sensitivity compared with other routine histological techniques (Herrero et
482 al., 2020). However, the sensitivity of CW was only 64% when compared to RT-rtPCR,
483 probably because the pre-sporogonic stages, which develop prior to the spores, are not
484 detected by CW. Assessment of *D. lepeophtherii* based on the presence of microvesicles
485 in gill tissue sections stained with H&E gave the lowest sensitivity (52%). Microvesicles
486 were only detected in 14 of the 28 fish examined, while the absence of *D. lepeophtherii*-
487 related necrosis was recorded in 8 fish. High burdens of *D. lepeophtherii* in tissue sections,
488 as denoted by Ct values below 19 and/or ISH total counts of over 100 microsporidia/10
489 mm² of gill tissue, were significantly associated with the development of the microvesicles
490 and these high burdens seem to be necessary for their formation. Microvesicles caused by
491 the microsporidian are probably the consequence of intense parasite proliferation and
492 spore formation and only obvious in the advanced and/or severe stages of the disease,
493 likely due to the release of the spores and disruption of fish cells. The presence of necrosis
494 of epithelial cells but absence of microvesicles, denoted in this study as foci of epithelial
495 cell necrosis, was suspected to be an early stage of the microvesicle formation.

496 Nevertheless, this change is non-specific and was not consistently associated with the
497 presence of a positive ISH signal. Although the presence of medium to high numbers of
498 microvesicles are highly suggestive of *D. lepeophtherii* infections in Atlantic salmon gills,
499 a positive RT-rtPCR or ISH result is necessary to confirm the presence of the parasite in
500 clinical cases.

501 The DNA-based ISH protocol developed during this study effectively detects *D.*
502 *lepeophtherii*, especially the pre-sporogonic phase, which does not label with other
503 histological techniques in Atlantic salmon in FFPE tissue sections. Therefore, this
504 technique enables assessment of parasite burden such that it correlates significantly with
505 the RT-rtPCR results in the absence of microvesicles which are present typically when the
506 *D. lepeophtherii* burden in gill tissue was very high, as determined by RT-rtPCR (Ct values
507 ≤ 19). Gill diseases are often complex and other pathology associated with the
508 microsporidian, such as epithelial cell necrosis, epithelial cell proliferation and
509 inflammation in the gills, is non-specific and can be associated with other infectious or
510 environmental factors. In addition, *D. lepeophtherii*-associated pathology changes during
511 disease progression (Matthews et al., 2013; Weli et al., 2017). Therefore, unless severe the
512 pathology caused specifically by *D. lepeophtherii* is difficult to discern in a complex gill
513 disease scenario by conventional H&E.

514 In conclusion, the ability of this newly developed ISH method to detect lesion-
515 associated *D. lepeophtherii* with very high sensitivity and specificity will provide valuable
516 information on the infection dynamics of the parasite. This will make it critical for studying
517 the progressive development and spread of *D. lepeophtherii* and possibly help establish a
518 suitable challenge model by either feeding fish infected tissue or cohabiting infected fish
519 with naïve fish. As this ISH protocol detects both spore types and the pre-sporogonic phase
520 of the parasite's infection in salmon gills and other tissues, it will enable a better

521 understanding of the parasite's life cycle and identification of the specific associated
522 pathology.

523

524 REFERENCES

525 Ahmed, N.H., Caffara, M., Sitjà-Bobadilla, A., Fioravanti, M.L., Mazzone, A., Aboulez, A.S.,
526 Metwally, A.M., Omar, M.A.E., & Palenzuela, O.R. (2019) Detection of the
527 intranuclear microsporidian *Enterospora nucleophila* in gilthead sea bream by *in situ*
528 hybridization. *Journal of Fish Diseases*, **42**(6), 809-815.

529 <https://doi.org/10.1111/jfd.12993>

530 Corthell, J. T. (2014) *In Situ* Hybridization. In *Basic Molecular Protocols in Neuroscience: Tips, Tricks, and Pitfalls* (pp. 105-111). San Diego, USA: Academic Press, Elsevier.

531 <https://doi.org/10.1016/B978-0-12-801461-5.00011-3>

532 Downes, J. K., Yatabe, T., Marcos-Lopez, M., Rodger, H. D., MacCarthy, E., O'Connor, I., Collins, E., & Ruane, N. M. (2018) Investigation of co-infections with pathogens associated with gill disease in Atlantic salmon during an amoebic gill disease outbreak.

533 *Journal of Fish Diseases*, **41**(8), 1217-1227. <https://doi.org/10.1111/jfd.12814>

534 Freeman, M. A. (2002) Potential biological control agents for the salmon louse *Lepeophtheirus salmonis* (Kroyer, 1837) (Doctoral dissertation). University of Stirling.

535 Freeman, M. A., & Sommerville, C. (2009) *Desmozoon lepeophtherii* n. gen., n. sp., (Microsporidia: Enterocytozoonidae) infecting the salmon louse *Lepeophtheirus salmonis* (Copepoda: Caligidae). *Parasites & Vectors*, **2**(1), 58.

536 <https://doi.org/10.1186/1756-3305-2-58>

537 Galván-Díaz, A. L., Magnet, A., Fenoy, S., Henriques-Gil, N., Haro, M., Gordo, F.P., Miró, G., del Águila, C., & Izquierdo, F. (2014) Microsporidia detection and genotyping study of human pathogenic *E. bienersi* in animals from Spain. *PLoS One*, **9**(3), e92289.

546 <https://doi.org/10.1371/journal.pone.0092289>

547 Georgiadis, M. P., Gardner, I. A., & Hedrick, R. P. (1998) Field evaluation of
548 sensitivity and specificity of a polymerase chain reaction (PCR) for detection of
549 *Nucleospora salmonis* in rainbow trout. *Journal of Aquatic Animal Health*, **10**(4), 372-
550 380. [https://doi.org/10.1577/1548-8667\(1998\)010<0372:FEOSAS>2.0.CO;2](https://doi.org/10.1577/1548-8667(1998)010<0372:FEOSAS>2.0.CO;2)

551 Gjessing, M. C., Spilsberg, B., Steinum, T. M., Amundsen, M., Austbø, L., Hansen, H.,
552 Colquhoun D., & Olsen, A. B. (2021) Multi-agent *in situ* hybridization confirms *Ca.*
553 *Branchiomonas cysticola* as a major contributor in complex gill disease in Atlantic
554 salmon. *Fish and Shellfish Immunology Reports*, **2**, 100026.
555 <https://doi.org/10.1016/j.fsirep.2021.100026>

556 Gjessing, M. C., Steinum, T., Olsen, A. B., Lie, K. I., Tavoranpanich, S., Colquhoun, D. J.,
557 & Gjevre, A. G. (2019) Histopathological investigation of complex gill disease in sea
558 farmed Atlantic salmon. *PLoS One*, **14**(10), e0222926.
559 <https://doi.org/10.1371/journal.pone.0222926>

560 Grésoviac, S. J., Baxa, D. V., Vivarès, C. P., & Hedrick, R. P. (2007) Detection of the
561 intranuclear microsporidium *Nucleospora salmonis* in naturally and experimentally
562 exposed chinook salmon *Oncorhynchus tshawytscha* by *in situ* hybridization.
563 *Parasitology Research*, **101**(5), 1257-1264. <https://doi.org/10.1007/s00436-007-0631-7>

564 Gunnarsson, G. S., Karlsbakk, E., Blindheim, S., Plarre, H., Imsland, A. K., Handeland, S.,
565 Sveier, H., & Nylund, A. (2017). Temporal changes in infections with some pathogens
566 associated with gill disease in farmed Atlantic salmon (*Salmo salar* L). *Aquaculture*, **468**,
567 126-134. <https://doi.org/10.1016/j.aquaculture.2016.10.011>

568 Herrero, A., Padrós, F., Pflaum, S., Matthews, C., del-Pozo, J., Rodger, H.D., Dagleish,
569 M.P., & Thompson, K.D. (2020) Comparison of histologic methods for the detection of

570 *Desmozoon lepeophtherii* spores in the gills of Atlantic salmon. *Journal of Veterinary*
571 *Diagnostic Investigation*, **32**(1), 142–146. <https://doi.org/10.1177/1040638719887707>

572 Herrero, A., Thompson, K. D., Ashby, A., Rodger, H. D., & Dagleish, M. P. (2018) Complex
573 gill disease: an emerging syndrome in farmed Atlantic salmon (*Salmo salar* L.). *Journal*
574 *of comparative pathology*, **163**, 23-28. <https://doi.org/10.1016/j.jcpa.2018.07.004>

575 Jones, S. R., Prosperi-Porta, G., & Kim, E. (2012) The diversity of microsporidia in parasitic
576 copepods (Caligidae: Siphonostomatoida) in the Northeast Pacific Ocean with
577 description of *Facilispora margolisi* ng, n. sp. and a new Family Facilisporidae n.
578 fam. *Journal of Eukaryotic Microbiology*, **59**(3), 206-217.
579 <https://doi.org/10.1111/j.1550-7408.2011.00614.x>

580 Luna, V. A., Stewart, B. K., Bergeron, D. L., Clausen, C. R., Plorde, J. J., & Fritsche, T. R.
581 (1995) Use of the fluorochrome Calcofluor White in the screening of stool specimens for
582 spores of microsporidia. *American Journal of Clinical Pathology*, **103**(5), 656-659.
583 <https://doi.org/10.1093/ajcp/103.5.656>

584 Martin, S. W. (1977) The evaluation of tests. *Canadian Journal of Comparative*
585 *Medicine*, **41**(1), 19 - 25.

586 Matthews, C. G. G., Richards, R. H., Shinn, A. P., & Cox, D. I. (2013) Gill pathology in
587 Scottish farmed Atlantic salmon, *Salmo salar* L., associated with the microsporidian
588 *Desmozoon lepeophtherii* Freeman et Sommerville, 2009. *Journal of Fish Diseases*,
589 **36**(10), 861-869. <https://doi.org/10.1111/jfd.12084>

590 Nylund, S., Andersen, L., Sævareid, I., Plarre, H., Watanabe, K., Arnesen, C.E., Karlsbakk,
591 E., & Nylund, A. (2011) Diseases of farmed Atlantic salmon *Salmo salar* associated with
592 infections by the microsporidian *Paranucleospora theridion*. *Diseases of Aquatic*
593 *Organisms*, **94**(1), 41-57. <https://doi.org/10.3354/dao02313>

594 Nylund, S., Nylund, A. R. E., Watanabe, K., Arnesen, C. E., & Karlsbakk, E. (2010).
595 *Paranucleospora theridion* n. gen., n. sp. (Microsporidia, Enterocytozoonidae) with a life
596 cycle in the salmon louse (*Lepeophtheirus salmonis*, Copepoda) and Atlantic salmon
597 (*Salmo salar*). *Journal of Eukaryotic Microbiology*, **57**(2), 95- 114.
598 <https://doi.org/10.1111/j.1550-7408.2009.00451.x>

599 Palenzuela, O., & Bartholomew, J. L. (2002). Molecular tools for the diagnosis of
600 *Ceratomyxa shasta* (Myxozoa). In *Molecular diagnosis of salmonid diseases* (pp. 285-
601 298). Springer, Dordrecht. https://doi.org/10.1007/978-94-017-2315-2_11

602 Pruesse, E., Quast, C., Knittel, K., Fuchs, B. M., Ludwig, W., Peplies, J., & Glöckner, F. O.
603 (2007) SILVA: a comprehensive online resource for quality checked and aligned
604 ribosomal RNA sequence data compatible with ARB. *Nucleic Acids Research*, **35**(21),
605 7188-7196. <https://doi.org/10.1093/nar/gkm864>

606 Rychlik W. (2007) OLIGO 7 primer analysis software. *Methods in Molecular Biology*
607 (*Clifton, N.J.*), **402**, 35–60. https://doi.org/10.1007/978-1-59745-528-2_2

608 Schoch, C. L., Seifert, K. A., Huhndorf, S., Robert, V., Spouge, J. L., Levesque, C. A., Chen,
609 W., & Fungal Barcoding Consortium. (2012) Nuclear ribosomal internal transcribed
610 spacer (ITS) region as a universal DNA barcode marker for *Fungi*. *Proceedings of the*
611 *National Academy of Sciences*, **109**(16), 6241-6246.
612 <https://doi.org/10.1073/pnas.1117018109>

613 Steinum, T., Kvellestad, A., Colquhoun, D. J., Heum, M., Mohammad, S., Grøntvedt, R. N.,
614 & Falk, K. (2010) Microbial and pathological findings in farmed Atlantic salmon *Salmo*
615 *salar* with proliferative gill inflammation. *Diseases of Aquatic Organisms*, **91**(3), 201-
616 211. <https://doi.org/10.3354/dao02266>

617 Stevens A., & Wilson I.G. (1996) The haematoxylin and eosin. In *Theory and*
618 *Practice of Histological Techniques* (p.99-112). Edinburgh, UK: Churchill Livingstone.

619 Stoecker, K., Dorninger, C., Daims, H., & Wagner, M. (2010) Double labelling of
620 oligonucleotide probes for fluorescence *in situ* hybridization (DOPE-FISH) improves
621 signal intensity and increases rRNA accessibility. *Applied Environmental*
622 *Microbiology*, **76**(3), 922-926. <https://doi.org/10.1128/AEM.02456-09>

623 Weli, S. C., Dale, O. B., Hansen, H., Gjessing, M. C., Rønneberg, L. B., & Falk, K. (2017)
624 A case study of *Desmozoon lepeophtherii* infection in farmed Atlantic salmon
625 associated with gill disease, peritonitis, intestinal infection, stunted growth, and
626 increased mortality. *Parasites & Vectors*, **10**(1), 370. [https://doi.org/10.1186/s13071-](https://doi.org/10.1186/s13071-017-2303-5)
627 [017-2303-5](https://doi.org/10.1186/s13071-017-2303-5)

628 Wilcox, J. N. (1993) Fundamental principles of *in situ* hybridization. *Journal of*
629 *Histochemistry & Cytochemistry*, **41**(12), 1725-1733.
630 <https://doi.org/10.1177/41.12.8245419>

TABLE 1. Sequences of *D. lepeophtherii* recovered from different host species and countries of origin, sequences were aligned to exclude variable regions in the oligonucleotide probe design. 16S small subunit (SSU) and internal transcribed spacer (ITS), 23S large subunit (LSU).

Accession Number	Number of bp	Target Gene	Host species/ Country
FJ594990	1885	SSU (partial)	Female sea lice <i>L. salmonis</i> / Norway
FJ389667	1656	SSU and LSU (partial); ITS;(complete)	Farmed Atlantic salmon / Norway
HM800847.2	1826	SSU (partial)	Farmed Atlantic salmon /Canada
AJ431366.2	1787	SSU; ITS; LSU (partial)	<i>L. salmonis</i> /Scotland
KR187183	1584	SSU (partial)	Wild rock cook wrasse (<i>Centrolabrus exoletus</i>)/ Norway
FJ594979	1559	SSU (partial)	<i>Caligus elongatus</i> / Norway
FJ594989	953	SSU (partial)	Farmed rainbow trout/ Norway
HM367691	685	SSU (partial)	Wild Atlantic salmon/ Norway

TABLE 2. Oligoprobe sequences specific for *Desmozoon lepeophtherii* designed for the *in situ* hybridization protocol. SSU = small subunit ribosomal ribonucleic acid, ITS = internal transcribed spacer, Tm = melting temperature of the probes. Results for individual oligoprobes in the optimised ISH protocol: - absence of labelling, + strong labelling, BL background labelling.

Name	Sequence 5'-3'	Region	Tm	Results
1284L21	CAAATCTGAACGTGATGCTAT	ITS	62.5°C	-
16L21	CGTTCCCCATTCGGTTCACAG	SSU	69.8°C	+
819L25	TTGCCCTCTCATGTCGCCAATCTA	SSU	74.4°C	+, BL
1002L25	ATATTTATGTCGCTCAAACGGATA	SSU	64.5°C	+
1339L25	ACACACTCACTAAGCAGTCCTACTA	ITS	69.1°C	+

TABLE 3. Formulae used to calculate the sensitivity and specificity of the various *Desmozoan lepeophtherii* detection techniques, using RT-rtPCR as reference.

Calculation	Formula
Sensitivity	$\frac{\sum \text{true positive results}}{\sum \text{true positive samples}} * 100$
Specificity	$\frac{\sum \text{true negative results}}{\sum \text{true negative samples}} * 100$
Positive predictive value	$\frac{\sum \text{true positive results}}{\sum \text{true and false positive results}} * 100$
Negative predictive value	$\frac{\sum \text{true negative results}}{\sum \text{true and false negative results}} * 100$

TABLE 4. Influence of different concentrations of reagents and variation in incubation times during optimisation of the ISH protocol. +/- weak signal, + strong signal, BL background labelling, SBL strong background labelling. Cocktail 1 (C1) consisted of probes 16L21, 819L25 & 1339L25. Cocktail 2 (C2) consisted of probes 1284L21, 1002L25 & 1339L25.

Step	Duration	Results
Proteinase K	15 $\mu\text{g mL}^{-1}$ 10 min	C1: +, BL
		C2: +
	15 $\mu\text{g mL}^{-1}$ 30 min	C1: +, BL
		C2: +
	No proteinase K	C1: +/-, BL
		C2: +/-
Pre-hybridization	30 min	C1: +, BL
		C2: +
	None	C1: +, BL
		C2: +
Stringency washes	2x SSC, 10 min 1x SSC, 10 min 0.5x SSC	C1: +, SBL
		C2: +
	10 min 2x SSC, 10 min 1x SSC, 10 min 0.25x SSC	C1: +, BL
		C2: +
Substrate incubation	3 h	C1: +, BL
		C2: +
	Overnight	C1: SBL
		C2: SBL

TABLE 5. Sensitivity, Specificity, Positive predictive value (PPV) and Negative predictive value (NPV) of the techniques used when compared with the RT- qPCR results for detecting the presence of *Desmozoon lepeophtherii* in salmon gills.

Method	Analysis	Results	Analysis	Results
<i>In situ</i> hybridization	Sensitivity	92.0%	PPV	100.0%
	Specificity	100.0%	NPV	60.0%
Calcofluor White	Sensitivity	64.0%	PPV	100.0%
	Specificity	100.0%	NPV	25.0%
Microvesicles (H&E)	Sensitivity	56.0%	PPV	100.0%
	Specificity	100.0%	NPV	21.4%

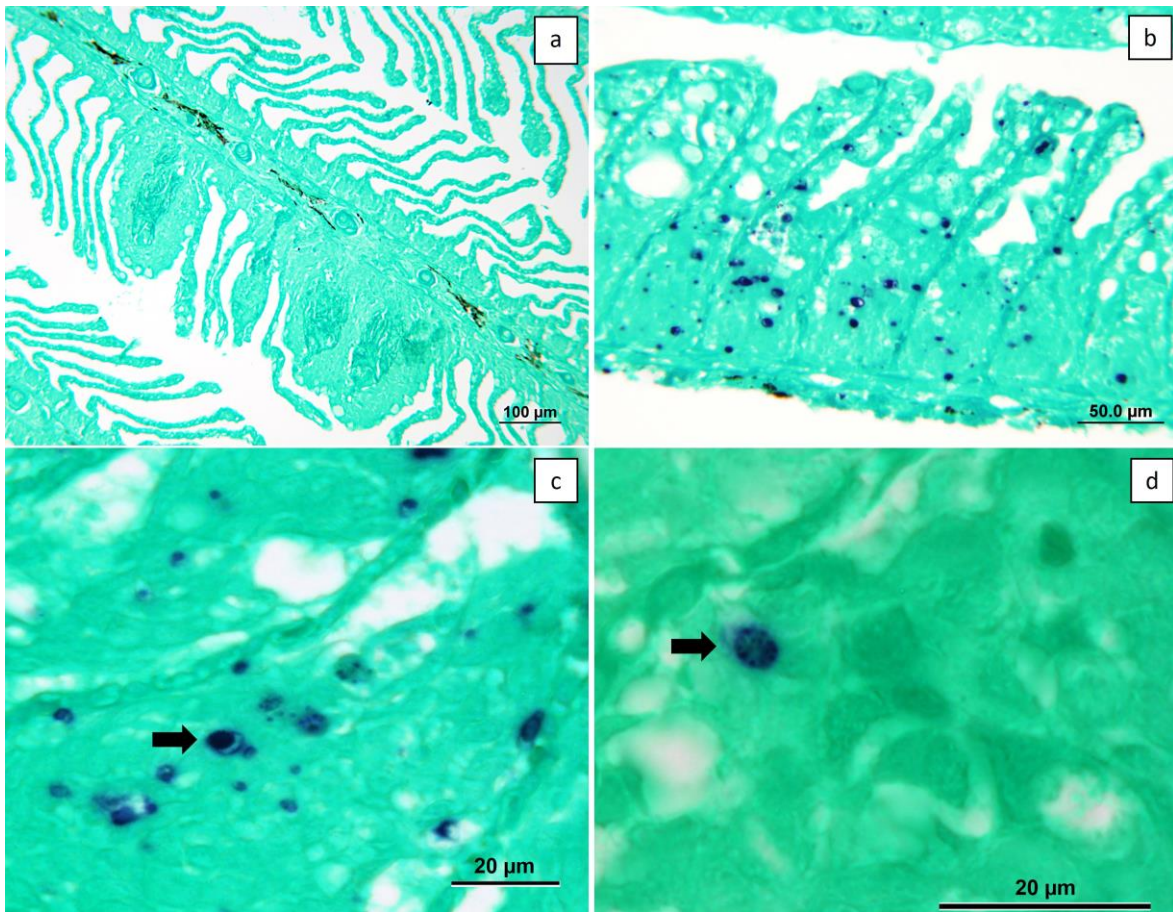


FIGURE 1. Atlantic salmon gill tissues subjected to *in situ* hybridisation specific for *Desmozoon lepeophtherii* (dark blue/purple pigment). (a) Negative for *D. lepeophtherii*, note section is devoid of labelling. There is melanin (dark brown pigment) in filament central venous sinus. (b) Positive, note pre-sporogonic stages present in the epithelial cells of the gill lamellae. Dark brown pigment in filament indicates melanin. (c) Positive, note the meront-like structure present (arrow) approximately 4 µm in diameter. (d) Positive, note sporont-like structure with punctate labelling that corresponds to forming spores.

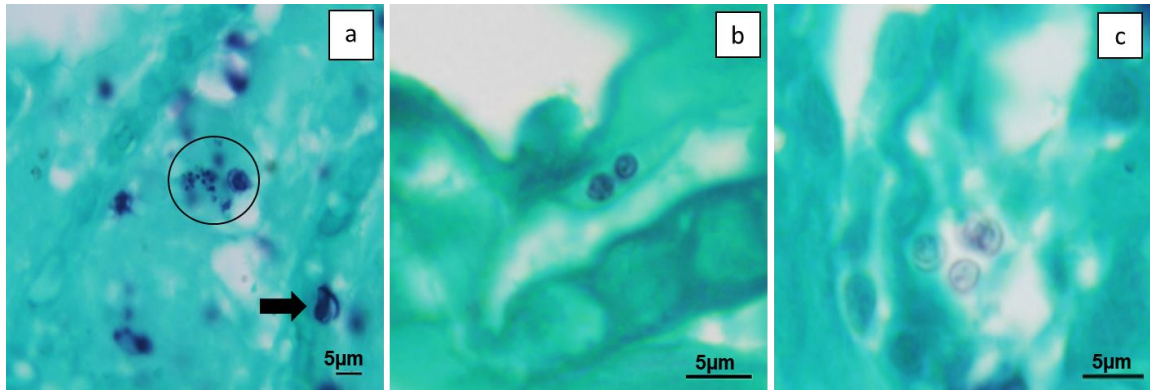


FIGURE 2. *In situ* hybridisation showing the presence of *Desmozoon lepeophtherii* in the gills of Atlantic salmon (dark blue/purple pigment). (a) Note proliferative stages (arrow) and a cluster of spore-like structures (circle) within the proliferating epithelium of the gill lamella; (b) Two labelled environmental spores; (c) A group of poorly labelled environmental spores of *D. lepeophtherii* measuring 2.5µm in diameter.

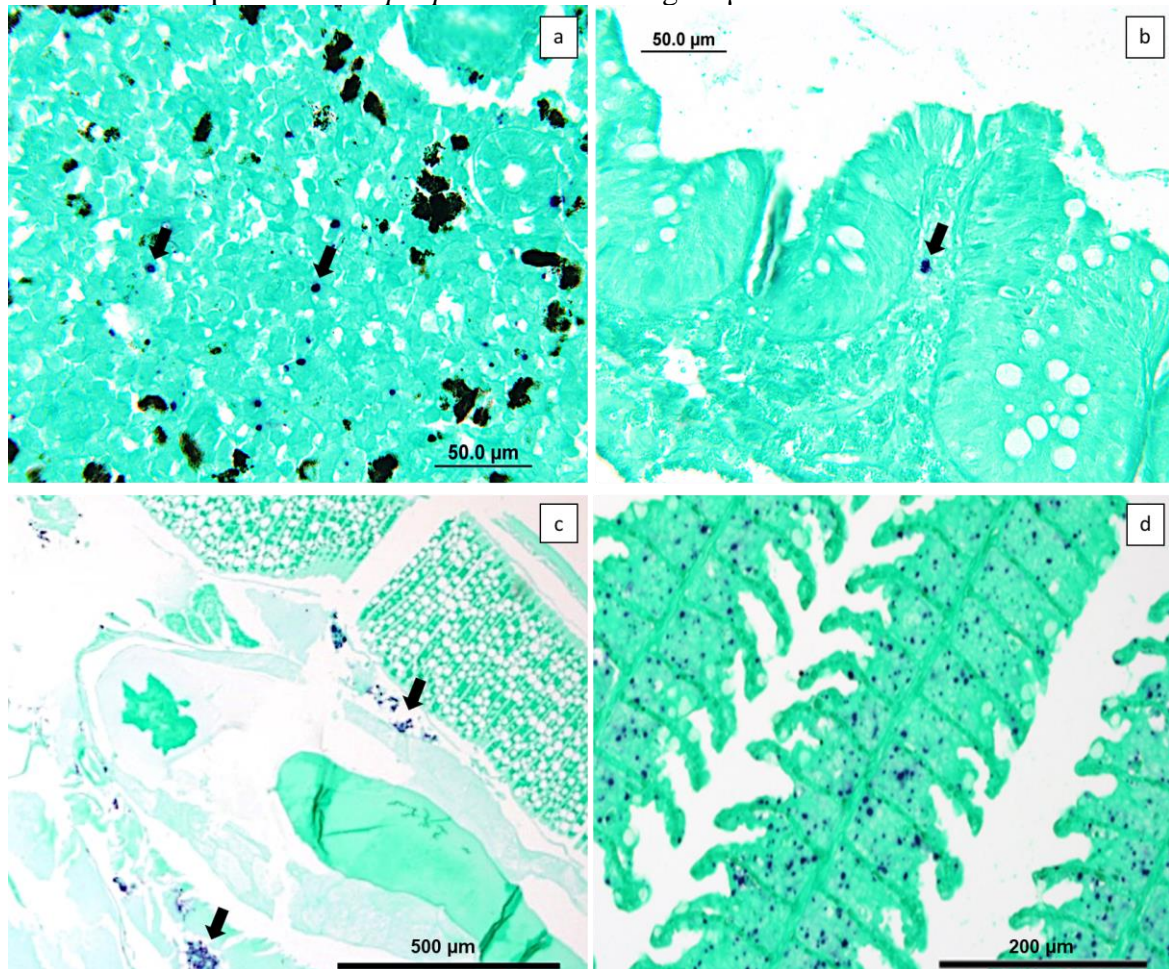


FIGURE 3. *In situ* hybridisation for *Desmozoon lepeophtherii* (dark blue/purple pigment) showing proliferative stages in (a) kidney interstitium (arrows) and (b) the *lamina propria* (arrow) of the intestine of Atlantic salmon; (c) sea louse (*Lepeophtheirus salmonis*) infected with *Desmozoon lepeophtherii* (arrows) and (d) gills from an Atlantic salmon from a salmon farm in Canada heavily infected with *D. lepeophtherii* (arrow). There is melanin (dark brown pigment) in kidney interstitium.

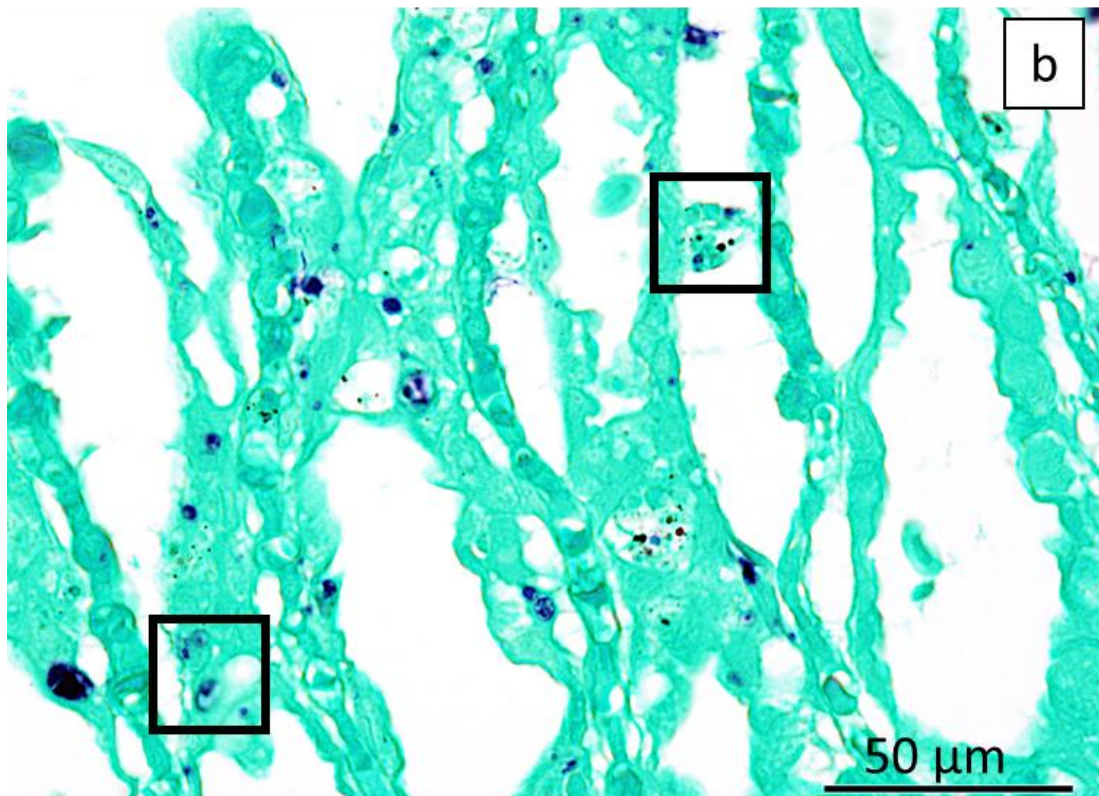
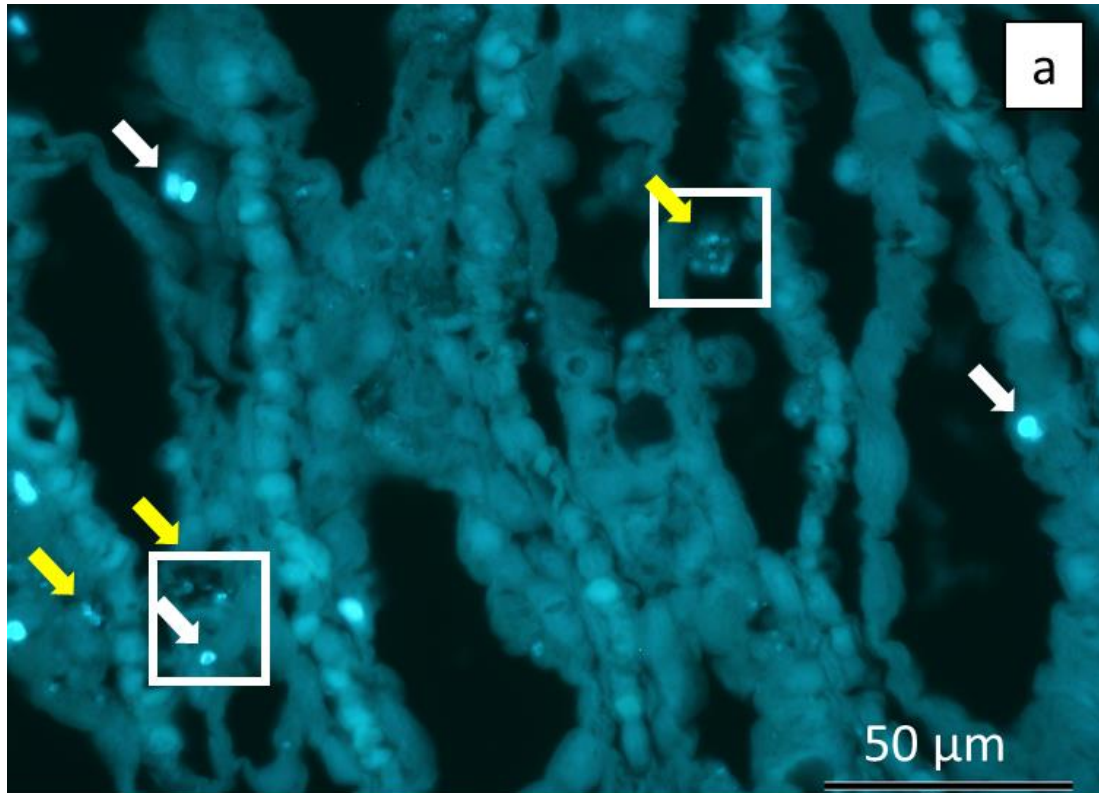


FIGURE 4. Semi-serial histological sections of gills of *Salmo salar* infected with *Desmozoon lepeophtherii*. (a) CW showing bright structures corresponding to large (white arrows) and small (yellow arrows) microsporidian spores, (b) note the same structures label (dark blue/purple pigment) with ISH (boxes).

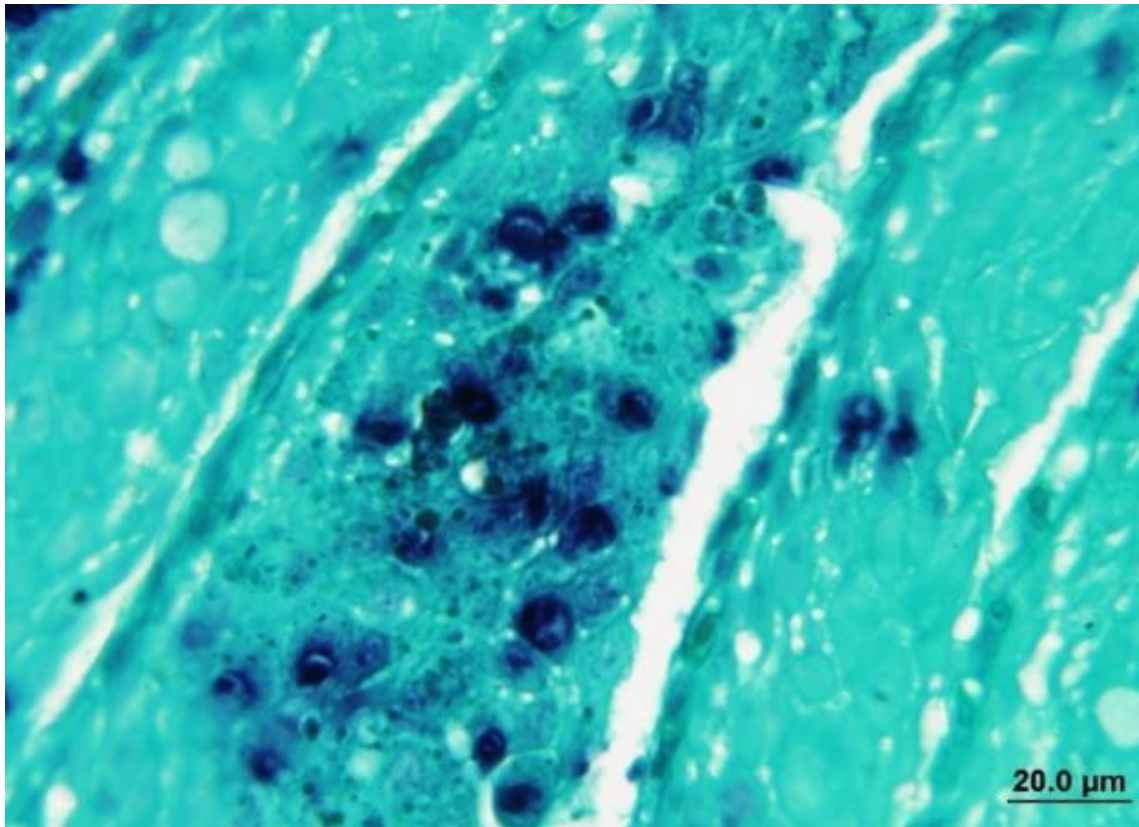


FIGURE 5. *In situ* hybridisation showing the presence of *Desmozoon lepeophtherii* (dark blue/purple pigment) in the gills of *Salmo salar* associated with a foci of epithelial cell necrosis.

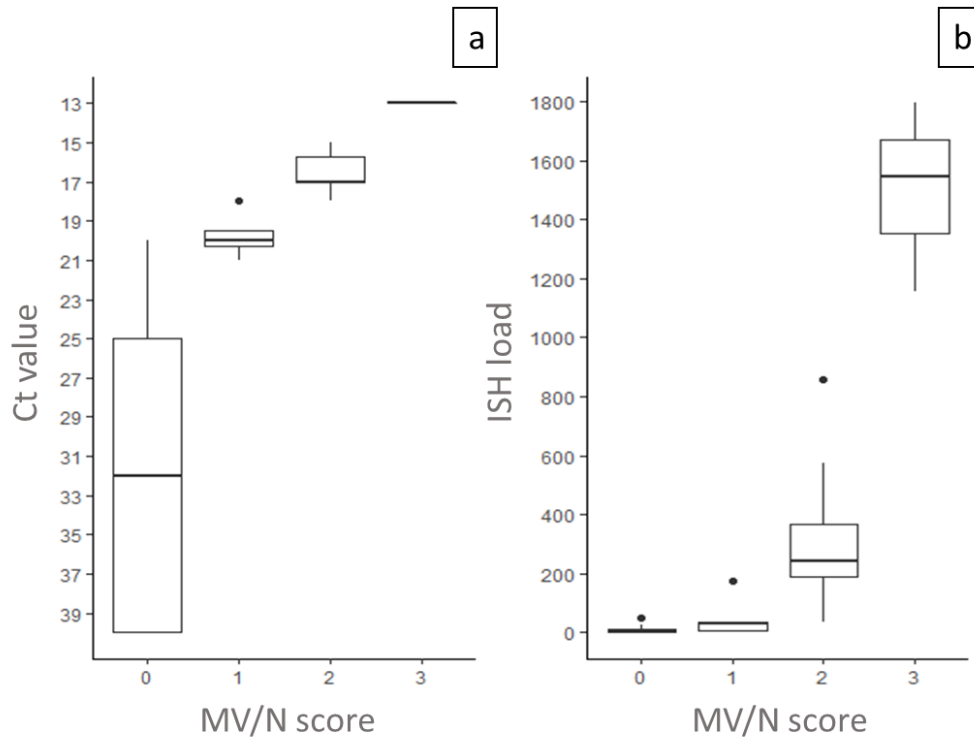


FIGURE 6. Boxplot of the microvesicle/necrosis score (MV/N) in salmon gill tissue with different burdens of *Desmozoan lepeophtherii* represented as (a) RT-rtPCR Ct values and (b) ISH total counts in 10 mm² of gill tissue (ISH load). Microvesicle/necrosis score (x-axis): 0 absence of necrosis, 1 epithelial cell necrosis but absence of microvesicles, 2 presence of small to medium numbers of microvesicles, 3 large numbers of microvesicles.